Journal of Power Sources 262 (2014) 488–493

Contents lists available at ScienceDirect

Journal of Power Sources

journal homepage: www.elsevier.com/locate/jpowsour

Carbon-supported Pt nanowire as novel cathode catalysts for proton exchange membrane fuel cells

Bing Li [a,b], Zeyu Yan [a,b], Drew C. Higgins [c], Daijun Yang [a,b,*], Zhongwei Chen [c], Jianxin Ma [a,b]

[a] School of Automotive Studies, Tongji University (Jiading Campus), 4800 Caoan Road, Shanghai 201804, China
[b] Cean Energy Automotive Engineering Center, Tongji University, Shanghai 201804, China
[c] Department of Chemical Engineering, University of Waterloo, Waterloo, Ontario, Canada N2L 3G1

HIGHLIGHTS

- Pt/C nanowire fabricated by a simple and inexpensive template-free methodology.
- Effect of different synthesis conditions investigated.
- Pt/C nanowire demonstrate significant ORR activity and durability.
- Free-template nanostructure control is highly effective for catalyst development.

ARTICLE INFO

Article history:
Received 17 February 2014
Received in revised form
21 March 2014
Accepted 1 April 2014
Available online 13 April 2014

Keywords:
Carbon-supported platinum nanowires (PtNW/C)
Durability
Oxygen reduction reaction (ORR)
Membrane electrode assembly (MEA)
Proton exchange membrane fuel cells (PEMFCs)

ABSTRACT

Carbon-supported platinum nanowires (PtNW/C) are successfully synthesized by a simple and inexpensive template-free methodology and demonstrated as novel, suitable cathode electrode materials for proton exchange membrane fuel cell (PEMFC) applications. The synthesis conditions, such as the amount of reducing agent and reaction time, were investigated to investigate the effect on the nanostructures and activities of the PtNW/C catalysts. High-resolution transmission electron microscopy (TEM) results show that the formic acid facilitated reduction is capable of producing uniformly distributed 1-dimensional PtNW with an average cross-sectional diameter of 4.0 ± 0.2 nm and length of 20–40 nm. Investigation of the electrocatalytic activity by half-cell electrochemical testing reveals that PtNW/C catalyst demonstrates significant oxygen reduction reaction (ORR) activity, superior to that of commercially available Pt/C. Using a loading of 0.4 mg_{Pt} cm^{-2} PtNW/C as the cathode catalyst, a maximum power density of 748.8 mW cm^{-2} in a 50 cm^2 single cell of commercial Pt/C. In addition, accelerated degradation testing (ADT) showed that the PtNW/C catalyst exhibits better durability than commercial Pt/C, rendering PtNW/C as a promising replacement to conventional Pt/C as cathode electrocatalysts for PEMFCs applications.

1. Introduction

Proton exchange membrane fuel cells (PEMFCs) are considered promising sustainable energy technologies owing to several advantages including high energy conversion efficiencies, quick startup times, transient performance capabilities, and zero by-product emissions at the point of operation [1]. These benefits render them highly attractive for application in vehicular propulsion, and for stationary or backup power. At the current status of PEMFC technology, there still remains a significant reliance on expensive Pt-based electrocatalysts. State of the art catalysts consist of platinum nanoparticles supported on high surface area carbon materials (Pt/C), that to date provide among the best catalytic activity toward the inherently sluggish oxygen reduction reaction (ORR). There, however, remains two key technical challenges that need to be addressed regarding the catalysts, particularly: (i) the ORR activity needs to be enhanced in order to reduce the overall expensive platinum loading at the cathode, and (ii) the long-term durability of the catalysts must be improved in order to extend the operational lifetimes of the membrane electrode assemblies (MEAs) [2]. Several different approaches have been employed to improve the ORR activity including alloying or

* Corresponding author. Clean Energy Automotive Engineering Center, Tongji University(Jiading Campus), 4800 Caoan Road, Shanghai 201804, China. Tel.: +86 21 6958 3891; fax: +86 21 6958 3850.
E-mail address: yangdaijun@tongji.edu.cn (D. Yang).

http://dx.doi.org/10.1016/j.jpowsour.2014.04.004
0378-7753/

nanostructure control strategies [3–11]. The latter technique has also been effective in improving electrocatalyst stability, whereby extended surface Pt and Pt–alloy structures have been demonstrated to results in increasing resistance to Pt rearrangement or dissolution [3–5]. Particularly, Pt-based nanowires (NW) [12], nanowire networks (NWNs) [13], nanoarrays (NA) [14] and Pt-coated nanostructured thin film (NSTF) "whiskers" [15] have recently been shown to provide activity or durability enhancements toward the ORR in comparison to conventional Pt/C. The activity enhancements are generally attributed to the increased number of high coordination number surface Pt atoms [16] or improved mass transport properties [17]; whereas the stability improvements result from the enhanced resistance to Pt dissolution due to the relatively lower surface energy of 1-dimensional nanostructures (i.e. NW) in comparison to 0-dimensional nanoparticles. These extended surface Pt NW catalysts are, however, commonly synthesized by complex and complicated hard template based techniques using silica or anodic aluminum oxide (AAO) [18], or relying on soft template methods using surfactants such as cetyltrimethylammonium bromide (CTAB) [13]. Template removal after synthesis is, however, an issue associated with these techniques and commonly requires the use of multi-step processes including hazardous chemicals such as hydrofluoric acid or highly caustic solutions. In addition, if the templates cannot be completely removed, it may severely affect the resulting electrocatalytic activities [19]. In this regard, utilizing template-free synthesis methods would be more suitable and flexible from a manufacturing perspective for the large-scale production of Pt-based electrocatalysts with controlled nanostructures for fuel cell applications [13]. Recently, Sun et al. [17,20–22] reported that Pt-based NWs could be synthesized by a template-free, formic acid based reduction technique. These materials were found to provide significantly improved specific and mass-based ORR activities, along with improved durability in comparison to Pt/C. These studies have relied on electrochemical half-cell investigations using aqueous 0.1 M $HClO_4$ electrolyte to evaluate ORR activity and stability capabilities, and currently no reports of electrode preparation, MEA integration and performance evaluations for Pt NW based catalysts exist. These studies are, however, highly pertinent and necessary in order to gauge the practical application potential of these new catalyst materials.

Herein, we synthesize carbon-supported platinum nanowires (PtNW/C) using the aforementioned formic acid reduction technique that is simplistic, inexpensive and template-free. The half-cell ORR activity and half-cell durability of these materials were optimized by investigating the effects of preparation parameters including the amount of reducing agent and reaction time, along with the resultant materials characterized using high-resolution transmission electron microscopy (TEM). The most promising reaction conditions were employed to prepare PtNW/C that were fabricated into unique electrode architectures and integrated into single cell MEAs for the first ever reported investigation of fuel cell performance and electrode stability.

2. Experimental

2.1. Materials and catalyst synthesis

PtNW/C were prepared by modifying a procedure reported previously [17]. In a typical synthesis, a mixed aqueous solution of $H_2PtCl_6 \cdot 6H_2O$ and 88% pure HCOOH, as well as an appropriate amount of carbon black (Vulcan XC72) were placed in a 100 mL glass beaker at room temperature. To achieve a loading of Pt on the carbon support of 40 wt. % Pt, 30 mL HCOOH and 0.15 g $H_2PtCl_6 \cdot 6H_2O$ were used in the synthesis. This corresponds to an HCOOH to $H_2PtCl_6 \cdot 6H_2O$ stoichiometric ratio of 2.4×10^3:1. When 20 mL of HCOOH is added, the corresponding stoichiometric ratio is 1.6×10^3:1, and when 40 mL of HCOOH is added, the corresponding stoichiometric ratio is 3.2×10^3:1. These precursors were dissolved in 50 mL ultrapure water; and then 75 mg of carbon black (Vulcan XC72) was dispersed in the above solution by ultrasonication (Model B25, BRT) for 60 min. The solution was then left stagnant and allowed to react for 72 h, after which the product was collected, washed and dried completely for further characterization. The resulting morphologies of the Pt-based catalysts prepared at different reaction times and reducing agent amounts were observed using TEM (JEOL 2010F). The quantity of Pt/C materials prepared at different conditions has been determined with inductively coupled plasma mass spectrometry (ICP-MS).

2.2. Electrochemical testing

For electrochemical evaluation, 4 mg of PtNW/C catalysts were suspended in 2 mL methanol/water/Nafion (40:10:1 wt%) solvent to prepare a catalyst ink, which was ultrasonicated (Model B25, BRT) for 2 h to ensure good catalyst dispersion. Then, 10 μL of the ink was deposited onto a clean glass carbon working ring disk electrode (RDE) (Model AFMSRCE, 6 mm diameter, Pine) twice and allowed to dry under ambient conditions. The overall loading of the mixed catalyst was 2.8×10^{-5} g cm^{-2}, and the ratio of catalyst to Nafion® polymer was 3:1 (in weight). PtNW/C catalysts were tested for their electrochemical ORR activity in a glass cell consisting of a three-electrode system in 0.1 M $HClO_4$ electrolyte at room temperature. A reversible hydrogen electrode (RHE) was used as the reference electrode, and Pt foil was used as the counter electrode. Cyclic voltammetry (CV) was carried out by six repeated cycles between 0.05 and 1.2 V vs RHE at a scan rate of 50 mV s^{-1}. Linear sweep voltammetry (LSV) was tested using three repeated cycles in a potential range of 0.05–1.20 V in the positive direction at a scan rate of 5 mV s^{-1} and electrode rotation speed of 1600 rpm [23,24]. The electrochemically active surface area (ECSA) and ORR half-wave potentials were calculated from the average of replicate testing, and standard deviations are listed in Table 2. Commercial 40% Pt/C (Johnson Matthey HiSpec 4000, JM) was also tested for comparison.

2.3. Membrane electrode assembly (MEA) fabrication

MEAs with an active area of 50 cm^2 were prepared using either PtNW/C or commercial Pt/C based cathodes. These electrodes were prepared by first dispersing PtNW/C (or Pt/C) in 5 wt.% Nafion® ionomer in isopropanol to form a catalyst ink. This ink was then directly sprayed using an automatic spraying system onto one side of a Nafion® 211 polymer membrane to form catalyst coated membrane (CCM). The ratio of catalyst to Nafion® polymer was 3:1. Spraying was controlled to result in a cathode catalyst layer Pt loading of 0.4 mg_{Pt} cm^{-2}. Anodes were prepared using Pt/C in the same fashion with a loading of 0.2 mg_{Pt} cm^{-2} [25]. The CCM was then fabricated into a 5-layer 50 cm^2 MEA by physically placing two pieces of gas diffusion layers (GDLs) (SGL, 24BC) on each side of the CCM.

Table 1
Element composition of Pt/C catalysts prepared at different amounts of reducing agent by ICP-MS.

Catalyst	Amount of reducing agent (mL)	Content/Pt (%)
Pt/C-20 mL	20	38.3
Pt/C-30 mL	30	38.8
Pt/C-40 mL	40	39.1

Table 2
Parameter of JM Pt/C and Pt/C catalyst prepared at different amounts of reducing agent.

Catalyst	ECSA ($m^2\ g^{-1}$)	MA ($mA/\mu g_{Pt}$)	SA ($mA\ cm^{-2}$)	Half-wave potential (V)
JM Pt/C	50 ± 0.2	0.064	1.41	–
Pt/C-20 mL	35 ± 0.2	–	–	0.862 ± 0.003
Pt/C-30 mL	41 ± 0.2	0.126	3.91	0.887 ± 0.003
Pt/C-40 mL	28 ± 0.2	–	–	0.822 ± 0.003

2.4. Single cell performance measurements

Single cell MEA tests were carried out for the fuel cell under steady state conditions. An electronic load was used for discharging and *I–V* discharge performances were carried out for the different electrode structures at 73 °C, and 0.1 MPa. The temperatures of the H_2 and air vapor feeds were maintained at 80 °C using tape heaters, and a relative humidity (RH) of 50% was maintained with bubbling humidifiers [26,27]. Reactant gas flow stoichiometries were fixed at 1.4 and 2.5 for H_2 and air, respectively.

3. Results and discussion

The catalyst synthesis parameters employed, such as reducing agent amount (HCOOH) and reaction time can significantly affect the structures and electrocatalytic activities of carbon-supported Pt catalysts for the ORR [1,28,29]. The reducing agent amount was varied from 20 to 40 mL, and the reaction time was varied from 48 to 96 h in order to determine their relative effect on the nanostructure and ORR activity of the synthesized PtNW/C.

3.1. Impact of reducing agent amount

Fig. 1 presents TEM images of the fabricated PtNW/C with the addition of varied reducing agent amounts. Fig. 1b illustrates the TEM image of the PtNW/C prepared with 30 mL of HCOOH, whereby it is clearly observed that the formic acid facilitated Pt reduction is capable of producing uniformly distributed 1-dimensional PtNW with an average cross-sectional diameter of 4.0 ± 0.2 nm and length of 20–40 nm. It was determined that by varying the amount of formic acid added, the distinct nanostructure and diameters of the PtNW can be modulated. When only 20 mL of formic acid is added, only Pt nanoparticles are formed most likely due to the fact that the Pt precursors were slowly reduced. When the amount of formic acid added is increased to 30 mL, and then further to 40 mL, PtNW are produced with increased average diameters, along with the appearance of partly agglomerated particles most likely due to the rapid rate of reduction at 40 mL. In order to accurately confirm the Pt loading on PtNW/C prepared with different amounts of reducing agent,

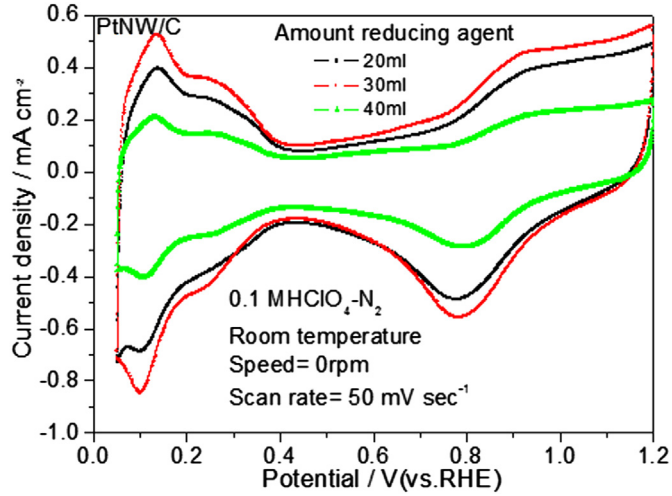

Fig. 2. CV curves of Pt/C prepared with different amounts of reducing agent in 0.1 M $HClO_4$ at the ambient solution temperature with a potential scan rate of 50 mV s^{-1}.

ICP-MS was employed with results provided in Table 1. It was found that the actual Pt loadings are similar to the calculated based on the amount of $H_2PtCl_6 \cdot 6H_2O$ in the reaction mixture.

Fig. 2 depicts the effects of formic acid amount on the CV curves of PtNW/C electrocatalysts. The charge transfer for hydrogen adsorption/desorption was used to calculate their electrochemically active surface areas (ECSA) listed in Table 2 to be 35 ± 0.2, 41 ± 0.2 and 28 ± 0.2 $m^2\ g_{Pt}^{-1}$ for PtNW/C formed with 20, 30 and 40 mL of formic acid, respectively. These values are similar to those reported in the literature [30]. Clearly the ECSA is maximized by employing 30 mL of formic acid, most likely due to the agglomeration along with the increased NW diameters at 40 mL of formic acid which could explain the slightly reduced ECSA. The amount of formic acid addition was also found to significantly affect the electrocatalytic activity of PtNW/C toward the ORR as displayed in Fig. 3. PtNW/C prepared with 30 mL of formic acid demonstrated superior ORR activity with respect to both onset and half-wave potentials. The half-wave potentials for the PtNW/C at 20 mL, 30 mL and 40 mL as displayed in Table 2 were 0.862 ± 0.003, 0.887 ± 0.003 and 0.822 ± 0.003 V, respectively, illustrating that the PtNW/C prepared with 30 mL of formic acid provides the highest activity through half-cell investigations.

3.2. The effect of reaction time on structures and catalytic activity of PtNW/C

It was found that the nanostructure of the PtNW/C and the cross-sectional diameters of the PtNW can also be tuned somewhat

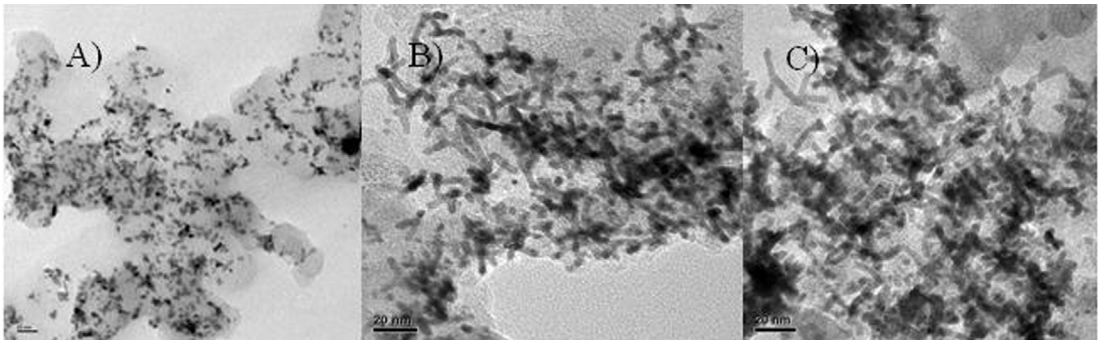

Fig. 1. TEM of Pt/C prepared with different amounts of reducing agent A) 20 mL, B) 30 mL, C) 40 mL.

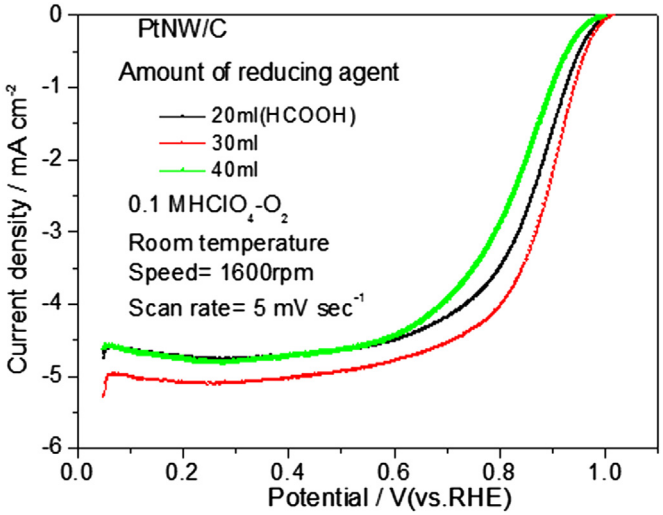

Fig. 3. LSV curves of Pt/C prepared with different amounts of reducing agent in 0.1 M $HClO_4$ at the ambient solution temperature with a potential scan rate of 5 mV s^{-1} and electrode rotation speed of 1600 rpm.

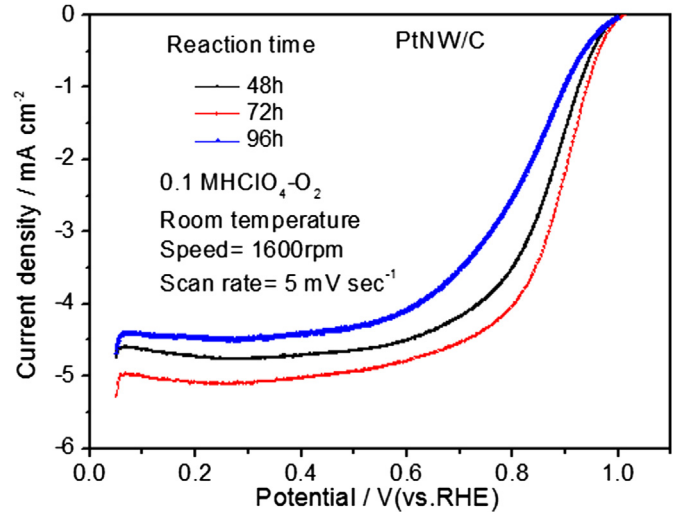

Fig. 5. LSV curves of Pt/C prepared with different reaction time in 0.1 M $HClO_4$ at the ambient solution temperature with a potential scan rate of 5 mV s^{-1} and electrode rotation speed of 1600 rpm.

by simply varying the reaction time. TEM images of PtNW/C prepared utilizing reaction times of 48 h, 72 h and 96 h are displayed in Fig. 4a–c, respectively. At 48 h of reaction time, PtNW start to form, and an increase in length is observed upon increasing the reaction time to 72 h. Upon further increasing the reaction time to 96 h, PtNW start to agglomerate at the base of growth on the carbon support.

We have also considered the effect of varying the reaction time on the ORR activity of PtNW/C catalysts as displayed in Fig. 5. From this figure, it can be seen that when the reaction time reaches 72 h, PtNW/C demonstrated superior ORR activity with respect to both onset and half-wave potentials. This is attributed to the fact that the PtNW/C catalyst formed well defined NW structures, which possess large surface areas, improving catalyst utilization and resulting in high activity.

It can be concluded that the nanostructure and ORR activity of the PtNW/C was ideal when using 30 mL of reducing agent and a reaction time of 72 h. These optimized materials were used subsequently for further electrochemical evaluations and MEA testing.

3.3. ORR activity and durability of PtNW/C compared to commercial Pt/C

Fig. 6A provides the ORR activity of PtNW/C in comparison to commercial Pt/C. Superior activity of PtNW/C was demonstrated in terms of both onset and half-wave potentials. Particularly, the half-wave potentials for the PtNW/C and Pt/C catalysts were 0.887 and 0.845 V, respectively. As shown in Fig. 6B and Table 2, PtNW/C exhibited a mass activity of 0.126 mA μg_{Pt}^{-1} at 0.9 V (vs. RHE), which is 1.97 times greater than that of Pt/C (0.064 mA μg_{Pt}^{-1}). From Fig. 6B, it also can be seen that the specific ORR activity for the PtNW/C is 3.90 mA cm_{Pt}^{-2} at 0.9 V, which is over twice that of commercial Pt/C catalyst (1.41 mA cm_{Pt}^{-2} at 0.9 V). This is attributed to the PtNW/C catalyst composed of highly coordinated surface Pt atoms which have higher inherent ORR activity due to reduced binding energies with oxygen containing species in comparison to the low surface coordinated Pt surface atoms present in nanoparticles. In addition, the preferential exposure of certain crystal facets of PtNW may be at play due to the varying activities that different low-index surface facets provide [17,31].

In order to investigate the stability of the catalyst materials, half-cell ADT was carried out. The catalyst coated electrode was subjected to 1500 potential cycles from 0.6 to 1.2 V vs RHE at a scan rate of 50 mV s^{-1} under nitrogen saturated conditions. Immediately following ADT, final CV curves were obtained in a similar fashion as outlined above. Fig. 7 presents CV curves before and after 1500 cycles of ADT for PtNW/C and commercial Pt/C. PtNW/C was found to have exemplary ECSA retention, maintaining 96.9% of the original ECSA. This was superior to commercial Pt/C, maintaining only 76.7% of the initial ECSA. This provides indication that the durability of PtNW/C is much better than commercial Pt/C.

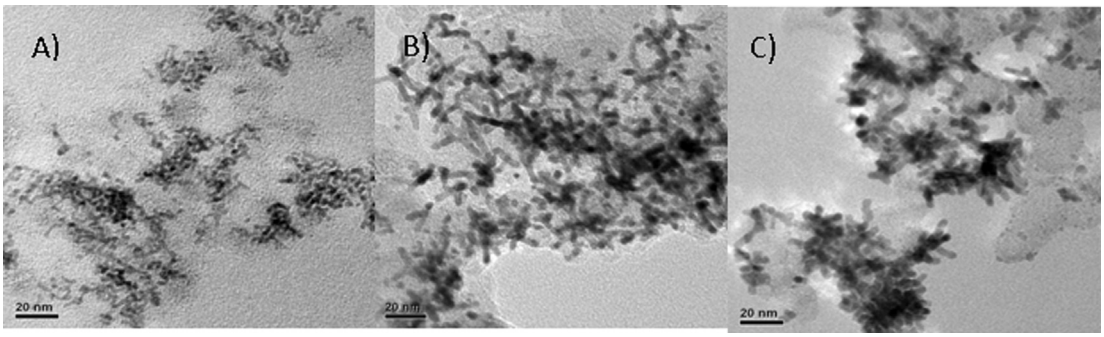

Fig. 4. TEM of Pt/C prepared with different reaction time (A) 48 h, B) 72 h, C) 96 h).

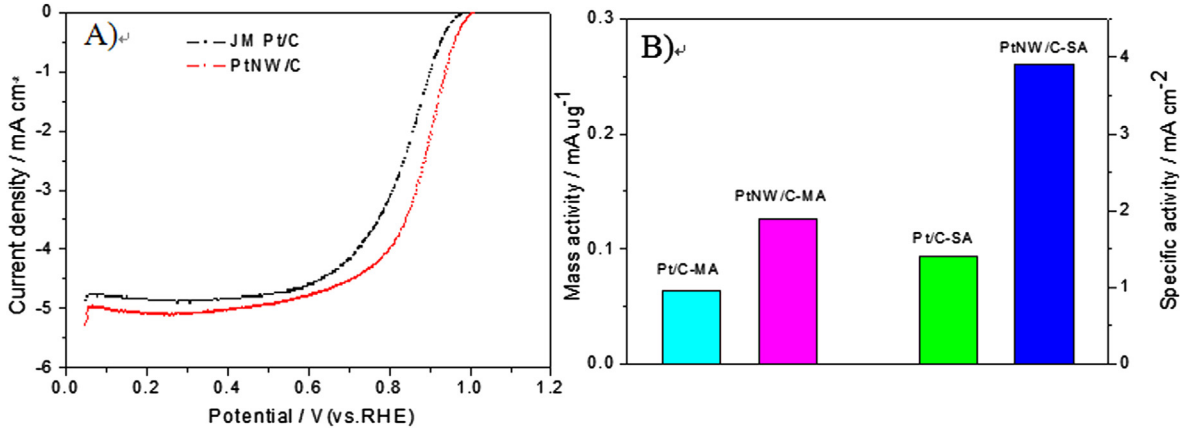

Fig. 6. A) LSV of PtNW/C and commercial Pt/C in 0.1 M $HClO_4$ at the ambient solution temperature with a potential scan rate of 5 mV s^{-1} and electrode rotation speed of 1600 rpm. B) Mass activity and specific activity at 0.9 V (vs. RHE) for the two catalysts.

Fig. 8 shows the MEA performance of PtNW/C based cathodes in comparison to commercial Pt/C. Prepared with cathode loadings of 0.4 mg_{Pt} cm^{-2}, PtNW/C produced a maximum power density of 748.8 mW cm^{-2}, an improvement over 715.4 mW cm^{-2} demonstrated by Pt/C under identical conditions. The improved cell performance for the NW compared with nanoparticles of Pt could be due to several factors, including: 1) the 1D (from 0D to 1D) shape could facilitate the reaction kinetics and improve the localized gas (O_2) transport thereby reducing activation polarization; 2) the unique PtNW/C nanostructures can be easily integrated into electrode architectures that adequately facilitate mass transport during operation and then reduce activation polarization, and 3) the extended surface structure of the PtNWs can weaken the interactions with oxygen containing species (i.e. OH_{ad}) and improve the ORR kinetics and cell performance [17,32]. This improved performance highlights the promise of using PtNW/Cs in advanced fuel cell electrode designs.

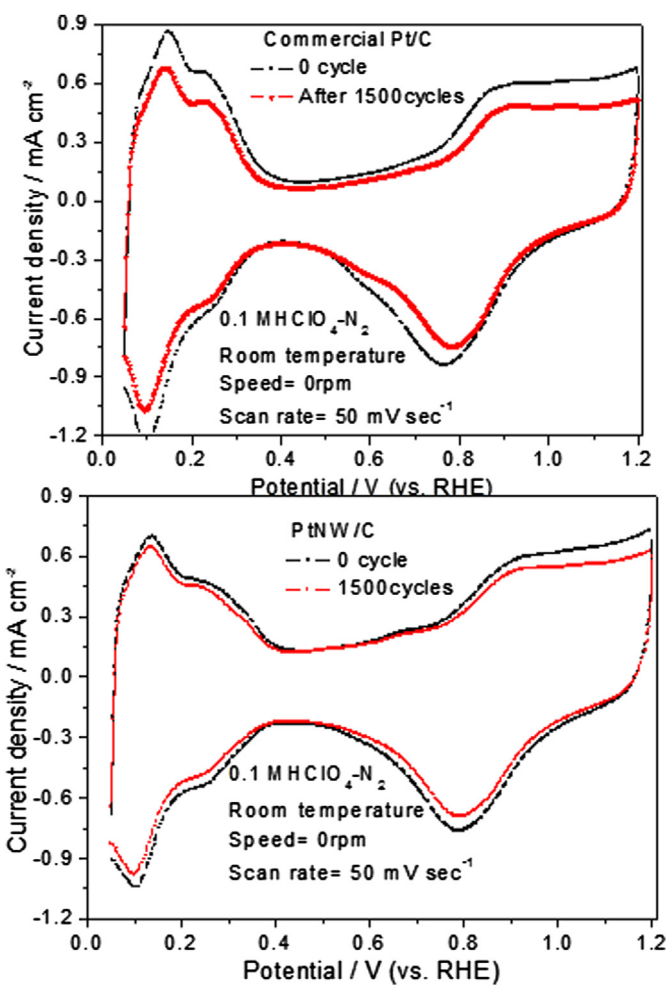

Fig. 7. CV curves of before and after 1500 cycles for PtNW/C and commercial Pt/C in 0.1 M $HClO_4$ at the ambient solution temperature with a potential scan rate of 50 mV s^{-1}.

4. Conclusions

In summary, PtNW/C have been successfully synthesized by a simple and inexpensive methodology for use as ORR electrocatalysts for fuel cell applications. Synthesis conditions, such as the amount of reducing agent and reaction time, were found to significantly affect the nanostructure of the PtNW/C catalysts. These 1D PtNW/C demonstrated significant ORR activity through half-cell testing, superior to that of commercially available Pt/C. The performance of an MEA prepared with a loading of 0.4 mg_{Pt} cm^{-2}

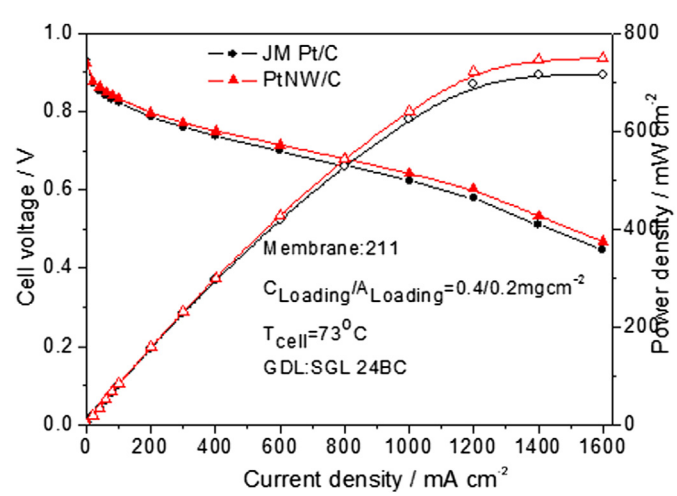

Fig. 8. Single cell performance curves using PtNW/C and commercial Pt/C under H_2/air conditions, Nafion 211, $C_{loading}/A_{loading}$ = 0.4 mg cm^{-2}/0.2 mg cm^{-2}, P = 0.1 MPa, RH = 50%.

PtNW/C as the cathode catalyst generated a maximum power density of 748.8 mW cm^{-2}, which is higher than that of commercially available Pt/C under the same conditions. In addition, the durability of PtNW/C by ATD was better than commercial Pt/C catalyst. With the results presented herein, PtNW/C material is presented as highly durable and active electrocatalyst materials for potential replacement of the commercial Pt/C as cathode catalysts for PEMFCs applications.

Acknowledgments

The authors appreciate the National Natural Science Foundation of China (No. 21206128), International Postdoctoral Exchange Fellowship Program China (201372) and China MoST (2012AA110501) for the financial support of this work. Also, this work was partly financed by Henkel Professorship of Tongji University.

References

[1] B. Li, D.C. Higgins, S.M. Zhu, H. Li, H.J. Wang, J.X. Ma, Z.W. Chen, Catal. Commun. 18 (2012) 51–54.
[2] S. Gottesfeld, T.A. Zawodzinski, Adv. Electrochem. Sci. Eng. 5 (1997) 195–301.
[3] B. Hwang, S. Kuma, C. Chen, M. Monalisa, D. Cheng, J. Liu, J. Phys. Chem. C. 111 (2007) 15267–15276.
[4] R. Narayanan, M. El-Sayed, Langmuir 21 (2) (2005) 027–2033.
[5] Z.W. Chen, M. Waje, W. Li, Y.S. Yan, Angew. Chem. Int. Ed. 46 (2007) 4060–4063.
[6] S. Kumar, S. Zou, Langmuir 23 (2007) 7365–7371.
[7] R. Narayanan, M. El-Sayed, J. Phys. Chem. B 108 (2004) 5726–5733.
[8] H. Yan, J. Song, H. Uchida, M. Watanabe, J. Phys. Chem. C. 112 (2008) 8372–8380.
[9] H. Gasteiger, N. Markovic, P. Ross, E. Cairns, J. Phys. Chem. 98 (1994) 617–625.
[10] V. Stamenkovic, B. Fowler, B. Mun, G. Wang, P. Ross, C. Lucas, N. Markovic, Science 315 (2007) 493–497.
[11] Z. Peng, H. Yang, J. Am. Chem. Soc. 131 (2009) 7542–7543.
[12] D.C. Higgins, S. Ye, S. Knights, Z.W. Chen, Electrochem. Solid-state Lett. 15 (2012) B83–B85.
[13] S.G. Wang, S.P. Jiang, X. Wang, J. Guo, Electrochim. Acta 56 (2011) 1563–1569.
[14] C.C. Chien, K.T. Jeng, Mater. Chem. Phys. 103 (2007) 400–406.
[15] M.K. Debe, J. Electrochem. Soc. 160 (2013) F522–F534.
[16] D.C. Higgins, J. Choi, J. Wu, A. Lopez, Z.W. Chen, J. Mater. Chem. 21 (2012) 3727–3732.
[17] S.H. Sun, G.X. Zhang, D.S. Geng, Y.G. Chen, R.Y. Li, M. Cai, X.L. Sun, Angew. Chem. Int. Ed. 50 (2011) 422–426.
[18] S.M. Choi, J.H. Kim, J.Y. Jung, E.Y. Yoon, W.B. Kim, Electrochim. Acta 53 (2008) 5804–5811.
[19] S.C. Yang, F. Hong, L.Q. Wang, S.W. Guo, X.P. Song, B.J. Ding, Z.M. Yang, J. Phys. Chem. C. 114 (2010) 203–207.
[20] S.H. Sun, F. Jaouen, J.P. Dodelet, Adv. Mater. 20 (2008) 3900–3904.
[21] S.H. Sun, D.Q. Yang, D. Villers, G.X. Zhang, E. Sacher, J.P. Dodelet, Adv. Mater. 20 (2008) 571–574.
[22] S.H. Sun, D.Q. Yang, G.X. Zhang, E. Sacher, J.P. Dodelet, Chem. Mater. 19 (2007) 6376–6378.
[23] B. Li, D.C. Higgins, D.J. Yang, H. Lv, Z.P. Yu, J.X. Ma, Int. J. Hydrogen Energy 38 (2013) 5813–5822.
[24] B. Li, D.C. Higgins, D.J. Yang, H. Lv, Z.P. Yu, J.X. Ma, Int. J. Hydrogen Energy 37 (2012) 18843–18850.
[25] B. Li, J.L. Qiao, D.J. Yang, R. Lin, H. Lv, H.J. Wang, J.X. Ma, Int. J. Hydrogen Energy 35 (2010) 5528–5538.
[26] B. Li, J.L. Qiao, D.J. Yang, J.S. Zheng, J.X. Ma, J.J. Zhang, H.J. Wang, Electrochim. Acta 54 (2009) 5614–5620.
[27] D.J. Yang, J.X. Ma, L. Xu, M.Z. Wu, H.J. Wang, Electrochim. Acta 51 (2006) 4039–4044.
[28] R. Wang, D.C. Higgins, M.A. Hoque, D.U. Lee, F. Hassan, Z.W. Chen, Sci. Rep. 3 (2013) 2431.
[29] D.C. Higgins, D. Meza, Z.W. Chen, J. Phys. Chem. C. 114 (2010) 21982–21988.
[30] B. Podlovechenko, G. Shterev, R. Semkova, E. Kolyadko, J. Electroanal. Chem. 224 (1987) 225–235.
[31] V.R. Stamenkovic, B. Fowler, B.S. Mun, G. Wang, P.N. Ross, C.A. Lucas, N.M. Markovic, Science 315 (2007) 490–493.
[32] J.L. Zhang, M.B. Vukmirovic, Y. Xu, M. Mavrikakis, R.R. Adzic, Angew. Chem. Int. Ed. 44 (2005) 2132–2135.